Eur. Phys. J. B **46**, 507–513 (2005)
DOI: 10.1140/epjb/e2005-00281-5

THE EUROPEAN PHYSICAL JOURNAL B

Raman scattering from GaP nanowires

M. Lamy de la Chapelle[1,2,a], H.X. Han[3], and C.C. Tang[2]

[1] Laboratoire de Nanotechnologie et d'Instrumentation Optique, Université de Technologie de Troyes, 12 rue Marie Curie, BP 2060, 10010 Troyes Cedex, France
[2] Nanostructures Laboratory, Tsinghua University, 100084 Beijing, P.R. China
[3] National Laboratory for Superlattices and Microstructures, Institute of Semiconductors, Chinese Academy of Sciences, Beijing 100083, P.R. China

Received 31 March 2005
Published online 7 September 2005 –

Abstract. A complete Raman study of GaP nanowires is presented. By comparison with the Raman spectra of GaP bulk material, microcrystals and nanoparticles, we give evidence that the Raman spectrum is affected by the one-dimensional shape of the nanowires. The Raman spectrum is sensitive to the polarization of the laser light. A specific shape of the overtones located between 600 and 800 cm^{-1} is actually a signature of the nanowires. Some phonon confinement and thermal behavior is also observed for nanowires.

PACS. 78.30.-j Infrared and Raman spectra – 63.22.+m Phonons or vibrational states in low-dimensional structures and nanoscale materials

1 Introduction

In recent years, one-dimensional (1D) semiconductor nanowires [1–3] with wide band gap, such as oxide [4,5], nitride [6,7] and phosphide [8], have attracted much attention because of their potential applications in photoelectronic devices and of interests in fundamental physics. The high aspect ratio (Lengths/Diameters) in 1D structures may give rise to anisotropy in the electronic and optical properties. The structural anisotropy in nanowire structures suggests some new aspects in lattice vibration properties. Considerable effort has been devoted to synthesize 1D-semiconductor structures and all of them have been extensively characterized by electron microscopy or X-ray diffraction. But few have really been studied by Raman spectroscopy [9–15]. In most cases, this latter technique is only used to determine the crystalline structure of the nanowires [1,2,4,6,7]. More recently, specific studies have been performed on Si [9,10], GaN [11], GaP [12–14] and ZnS [15] nanowires. It has been notably shown that the Raman features depends on the nanowires size [9,11] due to confinement effect and different nanowires diameter can be selectively excited by resonant Raman process as for carbon nanotube [16]. An alternative explanation to the Raman mode shift has been proposed by Mahan et al. [13]. Indeed, he introduces a new effect related to the particle shape. Thus, the large aspect ratio induces long range dipolar interaction in the nanowire and produces significant changes in the peak position. For GaP nanowires, it has been notably shown that the LO mode shifts of few cm^{-1}, whereas the TO mode frequency remains unchanged. Furthermore, new features can be observed for nanowires and they are assigned to surface optical (SO) phonons. Observed for GaP and ZnS nanowires [14,15], such SO phonons become Raman active due to the diameter modulation along the nanowires. Thus, the nanowire size, shape and structure induce actually specific Raman features and Raman scattering has been shown to be a powerful tool in characterizing 1D nanostructures (carbon nanotubes, nanowires). Whatever, even if polarization studies has been extensively performed on carbon nanotubes [17–19], less attention has been drawn to such studies for nanowires. In this report, we present detailed Raman scattering studies on polarization and confinement effect of phonon modes in GaP nanowires. We also show some thermal effects on such structures.

2 Experimental details

GaP nanowire samples used in this study are produced by carbon nanotube (CNT) template-confined growth method as reported in reference [8]. A mixture of Ga and Ga_2O_3 (4:1 as molar proportion) is used as a starting material to obtain Ga_2O, first. A mixture of Ga_2O, P and CNT with an appropriate proportion is then vacuum-sealed in a thick quartz tube and heated at 1000 °C for one hour in a furnace. During the GaP crystal growth, the chemical reaction between the gallium, the phosphorus and the carbon is confined all along the CNT. In

[a] e-mail: marc.lamy_de_la_chapelle@utt.fr

fact, the CNT serves as a template, which leads to a successful fabrication of one-dimensional GaP crystalline structures. The X-ray diffraction (XRD) measurements indicate that GaP nanowires are highly crystalline, and exhibit the cubic zinc blende structure of GaP preferentially grown along [001] direction. Transmission electron microscopy (TEM) characterization shows that the GaP nanowires have a wide diameter distribution ranged from 30 to 100 nm. The most of the GaP nanowires with a diameter no larger than 40 nm are single crystal while polycrystalline structure can also be seen for those with a diameter larger than 40 nm. Details on synthesis and characterization of GaP nanowires are described in a previous publication [8]. With a derived method, we can also obtain some samples with a high concentration of GaP nanoparticles with diameters of few nanometers.

Raman scattering studies were then performed on four different samples of GaP: bulk material, microcrystal (few micrometer in size), nanowires (NW) and nanoparticles (NP).

Raman scattering measurements are carried out at room temperature in back scattering geometry. A Jobin Yvon T64000 Raman spectrophotometer, equipped with an optical microprobe (×100 objective, numerical aperture: 0.90), was used. The spatial resolution is then close to 1 μm, and the spectral resolution is about 1 cm^{-1}. The excitation light source is the 514.5 nm line of an argon ion laser. For all experiments shown in Figures 1 to 4, a constant laser power of 600 μW at the focus of the microscope objective has been used, whereas the laser power was varied from 600 down to 100 μW for the power dependence study (Figs. 5 to 7).

For polarization study, the following direction has been chosen: Z-axis is the direction of the incident and scattered light (backscattering configuration). For bulk GaP cristal, Z-axis is perpendicular to the sample surface and corresponds to the [111] direction, whereas the X and Y are parallel to the sample surface and, respectively, to the $[10\bar{1}]$ and $[01\bar{1}]$ cristallographic directions. As uncertain orientation can be taken for reference coordinates in our nanowire or nanoparticle samples, we refer here the orientation of X as perpendicular to, and Y as parallel to the entrance slit of the Raman spectrometer. The incident light polarization is perpendicular to the Z-axis and is turned through 0 to 180 degrees, 0 degree corresponding to the X-axis. The polarization configurations are then called θX and θY, where X and Y coincide with the analyzed directions of the scattered light.

3 Results and discussion

In the Figures 1 to 3, we have plotted the Raman spectra recorded for the bulk material (a), microcrystal (b), nanowires (c) and nanoparticles (d). For all these spectra, the frequencies and assignment of the observed Raman bands are listed in Table 1.

Raman spectra of bulk crystalline GaP wafer (a) oriented along [111] crystal axis are depicted for comparison. In Raman scattering spectroscopy, GaP bulk crystals have

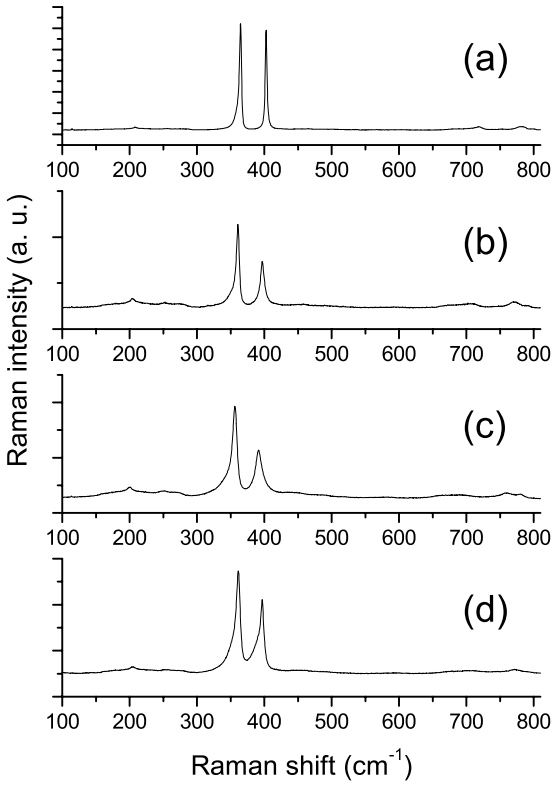

Fig. 1. Raman spectra of GaP samples for (a) bulk material, (b) microcrystal, (c) nanowires, (d) nanoparticles.

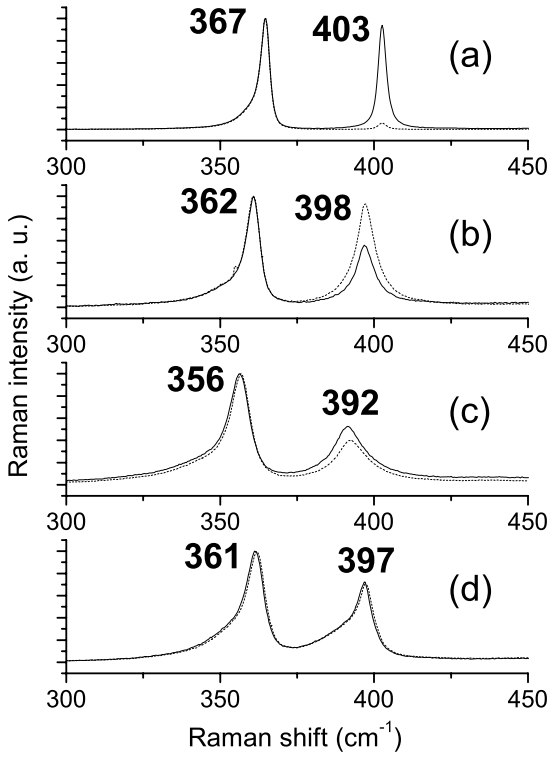

Fig. 2. Enlargement of the 300–450 cm^{-1} frequency range for (a) bulk material, (b) microcrystal, (c) nanowires, (d) nanoparticles. In solid line and dotted line are plotted the Raman spectra obtained for, respectively, the XX and the XY configuration.

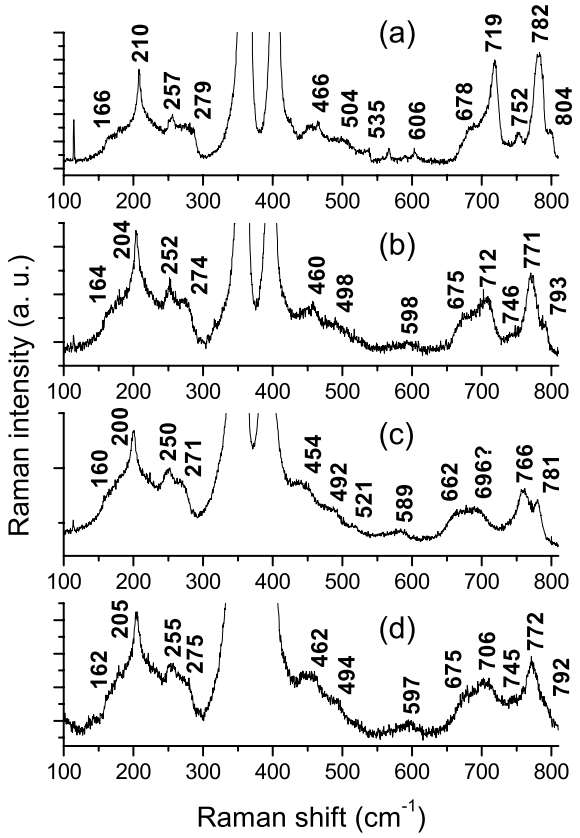

Fig. 3. Enlargement of overtones from 100 to 850 cm^{-1} for (a) bulk material, (b) microcrystal, (c) nanowires, (d) nanoparticles.

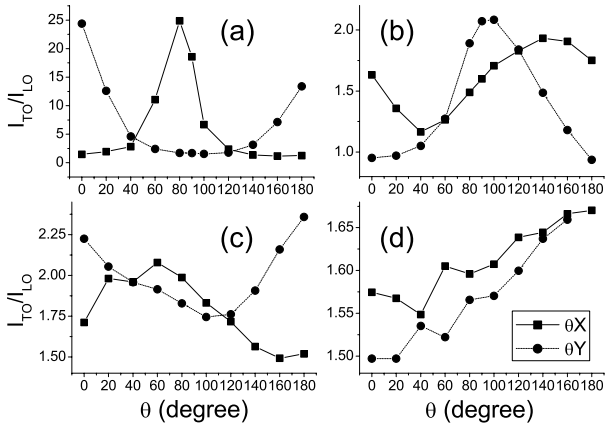

Fig. 4. Representation of the ratio ($I_{\mathrm{TO}}/I_{\mathrm{LO}}$) between the intensities of the TO mode and the LO mode versus the angle of polarization for (a) bulk material, (b) microcrystal, (c) nanowires, (d) nanoparticles.

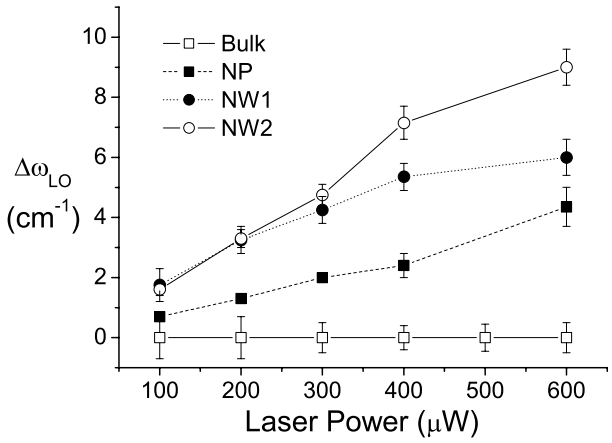

Fig. 5. Evolution of the shift of the LO mode ($\Delta\omega_{\mathrm{LO}}$) with the laser power for bulk material, nanowires (NW1 and 2) and nanoparticles (NP). Opened squares with plain line: bulk material, plain squares with dashed line: NP, plain circle with dotted line: NW1 and opened circle with plain line: NW2.

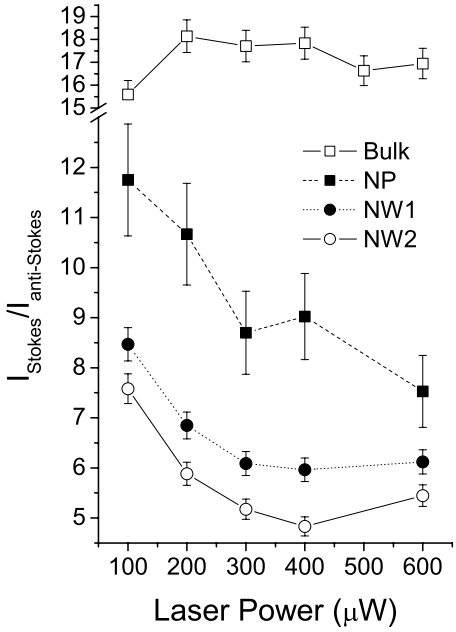

Fig. 6. Evolution of anti-Stokes/Stokes Raman intensity ratio ($I_{\mathrm{S}}/I_{\mathrm{AS}}$) with the laser power for bulk material, nanowires (NW1 and 2) and nanoparticles (NP). Opened squares with plain line: bulk material, plain squares with dashed line: NP, plain circle with dotted line: NW1 and opened circle with plain line: NW2.

been well characterized by TO and LO modes at 367 cm^{-1} and 403 cm^{-1}, respectively, and overtones and combined modes of acoustic and optical phonons, as shown in Table 1 [20–22].

By comparing the bulk Raman spectrum with the ones of other structures, we can, first, note that all the bands are downshifted to the low frequency range. This shift for the TO and LO modes may be of few cm^{-1} for the microcristal and the nanoparticles but more than 10 cm^{-1} for the nanowires. So, this shift depends on the studied structure and can be very large. We suppose that it is related to the shape and the size of the structures. But before to give an explanation of the existence of this shift, let us focus on the shape of the bands.

Indeed, nanowires (Figs. 2c and 3c) and nanoparticles (Figs. 2d and 3d) Raman spectra shows some wide broadening of all bands. In the case of the nanoparticles,

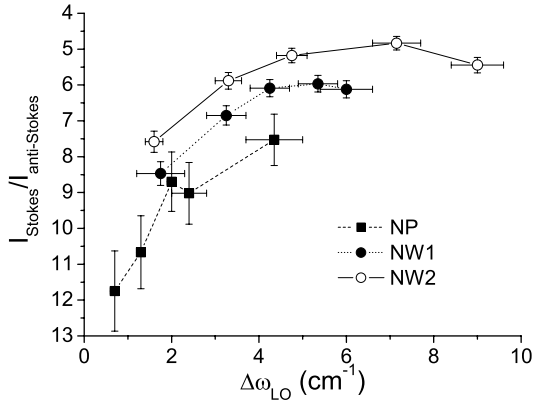

Fig. 7. Evolution of the shift of the LO mode ($\Delta\omega_{\mathrm{LO}}$) with anti-Stokes/Stokes Raman intensity ratio ($I_{\mathrm{S}}/I_{\mathrm{AS}}$). Plain squares with dashed line: NP, plain circle with dotted line: NW1 and opened circle with plain line: NW2.

a strong asymmetry on the low frequency side for the LO mode can also be observed. As no disordered phases have been observed by X-ray diffraction [8], we assume that this effect is probably due to the nanometric size of the particles. Some phenomenological models have shown that in finite-size nanocrystal, the relaxation of the $q = 0$ selection rules introduces changes in the vibration properties including a shift of the phonon frequency and an asymmetrical linewidth [23–25]. This confinement of the phonons occurs as well for optica [23–25] and acoustic modes [26–33] and have been extensively observed for semiconductor nanoparticles [23–38]. This suggests that the nanoparticles have clearly a diameter of few nanometers. On contrary, the nanowires bands are not so asymmetrical. This leads to deduce that the confinement effect is not so strong in the nanowires, as confirmed by their diameter of few tens of nanometer.

If we focus on the nanowire Raman spectrum, we can firstly note that no new feature is seen as observed by Gupta et al. [14] and assigned to SO phonons. It means that such phonons are not activated in our GaP nanowires. This gives evidence that their surface is very straight and no diameter modulation exists.

Moreover, the shape of the features between 600 and 800 cm^{-1} is remarkable and can not be assimilated to a GaP nanocrystal. Comparing to the bulk material (Fig. 3a), the microcrystal (Fig. 3b) and nanoparticles (Fig. 3d), the intensities of the 696 and 766 cm^{-1} modes are similar to the ones of the modes located at 662 and 781 cm^{-1}. This change is related to a decrease of the relative intensities of some specific modes and more especially the 2TO(X) and 2LO(X) modes (see Tab. 1). A decrease of the relative intensity of the LO(X)+TO(X) mode (close to 740 cm^{-1}) should have happened as this mode is no more observable. So it seems that the modes located on the X direction of the GaP Brillouin's zone are less favored than the ones of other directions. This is a first evidence of the existence of some preferential direction in the nanowires and it also gives evidence of a one-dimensional effect on the Raman spectrum.

A second evidence can be given by a polarization study. We have performed polarization experiments for each sample and recorded Raman spectra for various incident polarization angle to exhibit a possible existence of some directional effects [20,21]. Thus, the intensities of the optical modes are greatly dependent on the polarization of the incident and scattered light and on the direction inside the crystal. The intensity ratio between TO and LO modes is actually the most relevant signature of the orientation of the GaP species [20,21].

To estimate their intensities, the bands of the TO and LO modes are fitted by lorentzian bands. The TO mode has been fitted with two bands to take into account of its asymmetry on the low frequency side, which can be explain by a Fano effect [39]. To obtain its whole intensity, the intensities of the two lorentzians has been added. In Figure 4, we plot the $I_{\mathrm{TO}}/I_{\mathrm{LO}}$ ratio versus the angle θ between the X-axis and the polarization of the laser light (as explain before) and from its amplitude, we can appreciate the different behaviors of the different structures. The straight lines between the points are just plotted as a guide to follow the evolution of the $I_{\mathrm{TO}}/I_{\mathrm{LO}}$ ratio versus the angle and have no physical meaning.

For the bulk material, we observe a strong polarization effect with a large change of the relative intensity between the TO and LO modes. The θX and θY curves (Fig. 4a) have parabolic shape and are perfectly symmetric. Furthermore, the observation of an angle shift of 90 degrees of the θY comparing to the θX is what we expect for a perfect crystal with well-defined directions.

The closest spectrum to the bulk material is the one of the microcrystal. Except a sharp broadening of the TO and LO modes, all other bands are comparable (Figs. 2b and 3b) to the bulk ones. These few changes suggest us that the spectrum recorded is the one of well crystalline species with few disorder. Moreover, the LO line exhibits a strong intensity change between the (XX) and (XY) spectra. The polarization effect is not so high compared to the bulk material because of some misorientation of the crystalline structure.

In the case of the nanoparticles (Fig. 4d), we assume that the change of the $I_{\mathrm{TO}}/I_{\mathrm{LO}}$ ratio, near 0.1, is too low to be relevant of any polarization effect. It signifies that no preferential direction exists inside the studied area. We are in the case of a randomly distributed nanocrystals sample. The spectrum is then the combination of several crystals without the same orientations. The addition of all these different contributions results in an average Raman signal which eliminate any polarization effect.

In contrary, with the nanowires, we observe some clear polarisation effect (Fig. 4c). Whatever, this effect is different from the bulk material one. The curves no more show some parabolic shape and with the θY curve, it is possible to distinguish one main minimum at 100 degree and a local one at 40 degree. The θX curve presents also two maxima at 20 and 60 degree which do not correspond to the minima of the θY curve. All these accidents suggest that we do not observe only one preferential directions but several ones and each one contributes partially to the

Table 1. Assignments of all the observed bands, NO means that the mode as not been observed.

Assignment	Bulk material [9] (cm^{-1})	Microcrystal (cm^{-1})	Nanowires (cm^{-1})	Nanoparticles (cm^{-1})
TO(X)-LA(X)	104	NO	NO	NO
LA(X)-TA(X)	147	NO	NO	NO
$W_2^{"}$-W_1	166	164	160	162
2 TA(L)	182	NO	NO	NO
2 TA(X)	210	204	200	205
TO(X)-TA(X) / TO(L)-TA(L)	257	252	250	255
2 TA(K)	279	274	271	275
TO(Γ)	367	362	356	361
LO(Γ)	403	398	392	397
TO(L)+TA(L)	455	450	441	449
TO(X)+TA(X)	466	460	454	462
LO(X)+TA(X) / 2 LA(X)	504	498	492	494
$W_3^{'}$+$W_2^{"}$	535	532	521	NO
LO(L)+LA(L)	606	598	589	597
2 TO(K)	678	675	662	675
2 TO(L)	706	NO	NO	NO
2 TO(X)	719	712	696	706
LO(L)+TO(L)	738	NO	NO	NO
LO(X)+TO(X)	752	746	NO	745
2 LO(X)	782	771	766	772
2 LO(L)	786	NO	NO	NO
2 LO(Γ)	804	793	781	792

Raman signal. Thus, we assume that these preferential directions, observed with the polarisation effect, has to be assigned to the direction of the nanowires.

In summary, we can say that between the bulk material, the microcrystal and the nanoparticles, we just observe a change of the size of the crystal from the macroscopic to nanoscopic size. This change results in the broadening of the bands and the increase of the asymmetric shape of the TO and LO mode. For the nanowires, the broadening of the bands is also observed. But their one-dimensional structures have other consequences on the Raman spectrum: first, on the relative intensities of the overtones located between 600 and 800 cm^{-1} and second, on the behavior under polarized excitation. We think that all these specific behaviors are actually some signatures of the nanowires and can allow us to recognize them from nanoparticles or crystals.

Let us now focus on the shift observed for the bands. As described previously (see Tab. 1), all the modes show a decrease of their frequency. The shift of the peaks can go from 1 to 12 cm^{-1} for LO and TO modes. But it can be higher than 20 cm^{-1} for the overtones. As we study some nanostructures, this shift could be explained partly by the confinement of the phonon modes [23–25]. But the observed shift is too large and could not be only assigned to confinement, especially for the nanowires, since it has been predicted that with the same diameter, the nanowires shift should be lower than the nanoparticles one [24]. The shape effect has also to be considered [13]. But, as the confinement effect, the induced shift is too small compared to the 12 cm^{-1} and should only affect the LO modes. We have then searched the existence of another effect than the confinement to determine the origin of the shift.

Some research groups have reported the existence of a shift of the TO and LO modes when there is an excess of phosphorus in the GaP [40,41]. This shift is due to a distortion of the lattice parameters. But in this case, the shift is lower than 1 cm^{-1} and then two small to explain the one observed with our samples.

This shift could also be explained by a thermal effect probably due to a strongly focused laser beam. In this case, the increase of the atomic distance inside the material implies a softening of the phonon modes and then a decrease of their frequencies is observed here. In order to discriminate some thermal effect due to the laser illumination, we record Raman spectra of three zones: two containing nanowires, called NW1 and NW2, and one containing some nanoparticles, called NP, for several values of the laser power from 600 μW down to 100 μW. We do the same experiments with the bulk material to get a clear reference. Then, to get indication on the temperature of the different points, we also record the anti-Stokes spectra, as the intensity ratio between Stokes and anti-Stokes modes (I_S/I_{AS}) depends on this parameter. The lower intensity ratio is, the higher temperature is. To estimate the shift ($\Delta\omega_{LO}$) and the intensity ratio, we use the LO mode fitted by one lorentzian band.

As expected for this kind of behavior, we see, for the NP, NW1 and NW2, an increase of the shift with the laser power (Fig. 5) and a decrease of I_S/I_{AS} (Fig. 6). In the

opposite way, the LO mode of the bulk material show no shift and I_S/I_{AS} remains constant whatever the power is. This is a clear effect of the heating of the nanoparticles and nanowires by the laser power whereas the bulk material keeps the same temperature all along the experiments and can be taken as a reference. For each nanostructures, $\Delta\omega_{LO}$ can be explained by the thermal expansion of the lattice parameters.

But we can also note that the values and the evolution of the shift and the I_S/I_{AS} are different between NP and NW1 and 2. In the case of NP, for the same laser power, the I_S/I_{AS} is higher. The temperature and the shift are then lower than the ones obtained for NW1 and NW2 (Figs. 5, 6). A lower temperature implies that the heat is more diffused and more lost in the sample. So, it seems that the diffusion of the heat from the laser is more important for the nanoparticles than for the nanowires. As the nanostructures (nanowire and nanoparticle) are all smaller than the laser spot, no thermal loss can occur in a non exposed part of the structure, especially for nanowires. The nanowires could not loose any heat by conduction. The nanostructures could only decrease their temperature by thermal transfert to their close environnement and not inside their own structures. If so, this behavior can only be related to the diameter of the nanostructure. If we consider a lower diameter one, the surface/volume ratio is higher. In this way, the smallest nanostructure loses larger amount of heat. Its temperature should then be lower for a smaller diameter. This could explain the difference of temperature between the NP, with diameter of few nanometer and a spherical shape, and the nanowires, NW1 and NW2, with diameter around 40 nm and cylindrical shape. We can suppose that the differences between the NW1 and 2 temperatures is also due to the diameter difference. We can then suggest that the NW1 contains lower diameter (below 40 nm) nanowires, and the NW2 larger ones (above 40 nm).

Furthermore, as we can observe on the Figure 7, for NP, NW1 and 2, for the same I_S/I_{AS}, we find different values for $\Delta\omega_{LO}$. Thus, for the same temperature, $\Delta\omega_{LO}(NP) > \Delta\omega_{LO}(NW1) > \Delta\omega_{LO}(NW2)$. For the same temperature, we should have the same lattice parameter distortion and then if we suppose that the $\Delta\omega_{LO}$ is only due to thermal effect, we should expect the same shift. In order to explain the different $\Delta\omega_{LO}$, we assume the existence of another behavior for the shift. So the shift should be the addition of two effects: $\Delta\omega_{LO} = \Delta\omega_{ther} + \Delta\omega_2$, where $\Delta\omega_{ther}$ corresponds to the thermal shift constant for a fixed temperature and $\Delta\omega_2$ to a second one that we are going to determine. For a constant temperature, we observe that $\Delta\omega_{LO}(NP) > \Delta\omega_{LO}(NW1) > \Delta\omega_{LO}(NW2)$ and if we suppose that $\Delta\omega_{ther}(NP) = \Delta\omega_{ther}(NW1) = \Delta\omega_{ther}(NW2)$, we get $\Delta\omega_2(NP) > \Delta\omega_2(NW1) > \Delta\omega_2(NW2)$. Moreover, we have shown above that the size of the nanostructures increases from NP to NW2. Then, $\Delta\omega_2$ increases when the size decreases. We suggest that this second shift must be due to the confinement of the phonon modes. Indeed, as the structures studied have nanometric size, some confinement effect could occur and also implies a shift of the vibrational modes. This one increases when the diameter of the nanostructure decreases as we observe for $\Delta\omega_2$. Furthermore, $\Delta\omega_2$ can not be assigned to the shape effect as the TO mode frequency is shifted similarly than the LO modes [13]. This is in contradiction with such effect since only the LO mode should be shifted.

In summary, the shift of the bands is the addition of two different contributions: a thermal and a confinement effect such as $\Delta\omega_{LO} = \Delta\omega_{ther} + \Delta\omega_{conf}$.

One question, still opened in our discussion, concerns the thermal effect at 600 μW for the NW1 and 2 (Fig. 6). Indeed, at this power, I_S/I_{AS} is close to the one at 400 μW, which implies a stabilization of the temperature whereas the shift continues to increase with powers. This behavior is also different from the NP as the I_S/I_{AS} increases continuously with the power. We think it is not due to an experimental problem or to some large uncertainties since we can observe it for the two studied points NW1 and 2. We have not been able to determine the origin of this specific behavior and to give an available explanation of it. Whatever, this fact does not vanish our previous considerations on the thermal and confinement effects for lower power.

4 Conclusion

In this paper, we have studied GaP nanowires by Raman spectroscopy. After assignment of all the bands of the spectra, we have been able to determine the existence of some differences between the Raman spectra of nanowires, micro- and nanocrystals. We consider that the specific shape of the overtones between 600 and 800 cm^{-1} is a clear signature of the presence of nanowires in the studied area. This assumption has been confirmed by the observation of some polarization effect, allowed by the existence of preferential directions for the nanowires Moreover, we have observed a shift for all the bands visible on the Raman spectra. The origin of this shift has been interpreted as the addition of a thermal effect and a confinement of the vibrational modes inside the nanostructures.

This work has been partly supported by the National Natural Science Foundation of China (No. 6996030).

References

1. N. Wang, Y.H. Tang, Y.F. Zhang, C.S. Lee, I. Bello, S.T. Lee, Chem. Phys. Lett. **299**, 237 (1999)
2. Y.H. Tang, Y.F. Zhang, H.Y. Peng, N. Wang, C.S. Lee, S.T. Lee, Chem. Phys. Lett. **314**, 16 (1999)
3. K. Hiruma, M. Yazawa, T. Katsuyama, K. Okawa, K. Haraguchi, M. Kogucchi, H. Kakibayashi, J. Appl. Phys. **77**, 447 (1995)
4. H.Z. Zhang, Y.C. Kong, Y.Z. Wang, X. Du, Z.G. Bai, J.J. Wang, D.P. Yu, Y. Ding, Q.L. Hang, S.Q. Feng, Solid State Comm. **109**, 677 (1999)

5. D.P. Yu, Q.L. Hang, Y. Ding, H.Z. Zhang, Z.G. Bai, J.J. Wang, Y.H. Zou, W. Qian, G.C. Xiong, S.Q. Feng, Appl. Phys. Lett. **73**, 3076 (1998)
6. W. Han, S. Fan, Q. Li, Y. Hu, Science **277**, 128 (1997)
7. G.S. Cheng, S.H. Chen, X.G. Zhu, Y.Q. Mao, L.D. Zhang, Mat. Sci. Engineer. A **286**, 165 (2000)
8. C.C. Tang, S.S. Fan, M. Lamy de la Chapelle, H.Y. Dang, L. Peng, Adv. Mat. **12**, 1346 (2000)
9. W. Ding, L.Y. Li, B.B. Li, S.L. Zhang, Chin. Sci. Bull. **45**, 1351 (2000)
10. R. Gupta, Q. Xiong, C.K. Adu, U.J. Kim, P.C. Eklund, Nanoletters **3**, 627 (2003)
11. J. Zhang, L.D. Zhang, J. Phys. D: Appl. Phys. **35**, 1481 (2002)
12. Q. Xiong, R. Gupta, K.W. Adu, E.C. Dickey, G.D. Lian, D. Tham, J.E. Fischer, P.C. Eklund, J. Nanosci. Nanotech. **3**, 335 (2003)
13. G.D. Mahan, R. Gupta, Q. Xiong, C.K. Adu, P.C. Eklund, Phys. Rev. B **68**, 073402 (2003)
14. R. Gupta, Q. Xiong, G.D. Mahan, P.C. Eklund, Nanoletters **3**, 1745 (2003)
15. Q. Xiong, J.G. Wang, O. Reese, L.C. Lew Yan Voon, P.C. Eklund, Nanoletters **4**, 1991 (2004)
16. A.M. Rao, E. Richter, S. Bandow, B. Chase, P. Ek-lund, K. Williams, S. Fang, K. Subbaswamy, M. Menon, A. Thess, R.E. Smalley, G. Dresselhaus, M.S. Dresselhaus, Science **275**, 187 (1997)
17. A. Jorio, A.G. Souza Filho, V.W. Brar, A.K. Swan, M.S. Unlu, B.B. Goldberg, A. Righi, J.H. Hafner, C.M. Lieber, R. Saito, G. Dresselhaus, M.S. Dresselhaus, Phys. Rev. B **65**, R121402 (2002)
18. A. Jorio, G. Dresselhaus, M.S. Dresselhaus, M. Souza, M.S. Danta, M.A. Pimenta, A.M. Rao, R. Saito, C. Liu, H.M. Cheng, Phys. Rev. Lett. **85**, 2617 (2000)
19. J. Azoulay, A. Débarre, A. Richard, P. Tchénio, S. Bandow, S. Iijima, Chem. Phys. Lett. **331**, 347 (2000)
20. R.M. Hoff, J.C. Irwin, Can. J. Phys. **51**, 63 (1973)
21. M.M. Sushchinsky, V.S. Gorelik, O.P. Maximov, J. Raman Spectroscopy **7**, 26 (1978)
22. B. Pödör, Phys. Stat. Sol. (b) **120**, 207 (1983)
23. H. Richter, Z.P. Wang, L. Ley, Solid State Commun. **39**, 625 (1981)
24. I.H. Campbell, P.M. Fauchet, Solid State Commun. **58/10**, 739 (1986)
25. K. Huang, B.F. Zhu, H. Tang, Phys. Rev. B **41**, 5825 (1990)
26. A. Tamura, K. Higeta, T. Ichinokawa, J. Phys. C: Solid State Phys. **15**, 4975 (1982)
27. N. Nishiguchi, T. Sakuma, Solid State Commun. **38**, 1073 (1981)
28. E. Duval, A. Boukenter, B. Champagnon, Phys. Rev. Lett. **56/19**, 2052 (1986)
29. M. Fujii, T. Nagareda, S. Hayashi, K. Yamamoto, Phys. Rev. B **44**, 6243 (1991)
30. A. Tanaka, S. Onari, T. Arai, Phys. Rev. B **47**, 1237 (1993)
31. M. Fujii, Y. Kanzawa, S. Hayashi, K. Yamamoto, Phys. Rev. B **54**, R8373 (1996)
32. L. Saviot, B. Champagnon, E. Duval, A.I. Ekimov, Phys. Rev. B **57**, 341 (1998)
33. L. Saviot, B. Champagnon, E. Duval, I.A. Kudriavtsev, A.I. Ekimov, J. Non-Crystalline Solid **197**, 238 (1996)
34. M. Fujii, S. Hayashi, K. Yamamoto, Appl. Phys. Lett. **57/25**, 2692 (1990)
35. M. Fujii, S. Hayashi, K. Yamamoto, Jpn. J. Appl. Phys. **30/4**, 687 (1991)
36. A. Tanaka, S. Onari, T. Arai, Phys. Rev. B **45**, 6587 (1992)
37. Z. Iqbal, S. Veprek, A.P. Webb, P. Capezzuto, Solid State Commun. **37**, 993 (1981)
38. P. Mishra, K.P. Jain, Phys. Rev. B **62**, 14790 (2000)
39. P. Galtier, V. Lemos, M. Zigone, G. Martinez, Phys. Rev. B **28**, 7334 (1983)
40. Y. He, N.A. El-Masry, J. Ramdani, S.M. Bedair, T.L. McCormick, R.J. Nemanich, E.R. Weber, Appl. Phys. Lett. **65**, 1673 (1994)
41. K. Kuriyama, T. Kato, S. Tajima, T. Kato, S.-I. Takeda, Appl. Phys. Lett. **66**, 2995 (1995)